Comparison of Hardness Values of Various Specimens with Different Geometries and Material Properties after ECAP

Mohammad Hossein Shahsavari[1], Farshid Ahmadi[2*]
[1]Department of Mechanical Engineering, Najafabad Branch, Islamic Azad University, Najafabad 8514143131, Iran
[2]Department of Mechanical Engineering, Isfahan University of Technology, Isfahan 84156-83111, Iran,
[*]E-mail of corresponding author: fahmadi@me.iut.ac.ir
Received: March 27, 2015; Accepted: May 23, 2015

Abstract
Nowadays, equal channel angular pressing, known as the ECAP process, is one of the most popular methods for manufacturing ultra-fine grained (UFG) materials. In this paper, Ecap process has been carried out on pure copper and 6012 aluminum alloy up to six passes by route B_C. Principal attention was paid to the influence of parameters such as diameter, material, and the height of billet on mechanical properties and hardness homogeneity induced by the process. Moreover, microhardness measurements carried out on the cross-section of the ECAPed copper and aluminum showed 103 and 46 % increase in hardness magnitude and 115 and 50% in S_{UT} after the sixth pass. Furthermore, hardness distribution got better for AA6012 and worse for copper after six passes of ECAP. Finally, a computer program was used to obtain effective strain distribution imposed to across the width at the center of the samples after one pass. The results obtained from the 3D FEM method were compared with the hardness measurement and showed good conformity with experimental results, which indicated that homogeneity strain improves as increasing the diameter and height had no conspicuous effect on value and homogeneity of strain and hardness of the central region of specimens.

Keyword:
ECAP, Aluminum alloy, Pure copper, 3D FEM, Strain homogeneity

1. Introduction

Severe plastic deformation (SPD) is a popular method for producing ultra-fine grained materials and has attracted wide attention because of unique mechanical properties obtained by this procedure [1,2]. ECAP is one of the usual ways and probably the best of SPD processes that extrudes samples through a die with specific geometric features. ECAP was first introduced as a potential processing method by Segal [3,4]. This procedure has enormous advantages in comparison with other techniques like rolling, because intense plastic strains can be imposed without any change in the cross-section dimension of the sample. Therefore, highly desired strains could be achieved by repeating the process and improving toughness and strength of metallic materials[2]. During ECAP, a sample is pressed through two intersecting channels with the same cross sections. The schematic diagram of the ECAP die is shown in Figure 1. The angle between the channels and the outer corner angle are defined by Φ and Ψ, respectively. There are four fundamental routes that are shown in Figure 2. The difference between them is in the activation of the slip system [5]. In route A, there is not any rotation. In route C, the sample rotates 180°after each pass. In routes B_A and B_c, a 90° rotation in an alternate direction and in the

same direction is applied to the sample between consecutive passes [6]. The true achieved strain of ε_N by ECAP can be related to the number of passes N, the channel angle of Φ and the curvature radius at the outer corner Ψ by Eq.1[7]:

$$\varepsilon_N=\frac{1}{\sqrt{3}}\sum_{i=1}^{N}\left(\left(2\ \cot(\frac{\Phi+\Psi}{2})\ \right)+\Psi\ \mathrm{cosec}\ (\frac{\Phi+\Psi}{2})\ \right) \quad (1)$$

Eq. (1) does not present the local deformation behavior or the homogeneity of strain distribution in the cross-section of the sample that is noticed in experimental work.

In recent years, numerous theoretical and experimental investigations have been conducted on the ECAP process to demonstrate the effect of process parameters on material behavior. For example, Sordi et al. [8] presented experimental and FEM results and evaluated the relationships between the ECAP die design, strain distribution and pressing forces.

An immense number of FEM works were performed to analyze the plastic deformation behavior of the process with various die parameters [9-15]. All of them analyzed strain distribution of ECAP after one pass. Most of the FEM works on ECAP have been modeled as 2D plane strain. Several parameters were considered in the simulations. For example, the plastic deformation behavior of the billet during ECAP was performed by Kim et al. [16]. The effect of die geometry on the effective strain was explored in some papers like Han et al. and Nagasekhar et al. [17,18]. Nagasekhar [18] showed that acute tool-angles in ECAP can increase the strain induced in the material within minimum number of passes. Oruganti et al. [19] reported the influence of backpressure, friction and strain rate sensitivity on the ECAP process. They found that friction had different behavior in distinct temperature conditions. They concluded that although a moderate amount was beneficial at room temperature, friction had a negative interaction with strain rate sensitivity at high temperature. Despite the fact that backpressure had large useful effects, it had negative effects when combined with friction and high strain rate sensitivity. Xu et al. [20] surveyed the effect of different die channel angles and corner angles on effective strain in the main deformation zone of the work-piece during ECAP. The studies of Yoon et al. [21] on the ECAP process were aimed to identify the influential parameters which cause the bending of the work-piece during the ECAP process. Their results showed that strain rate sensitivity plays an important role on homogeneity of the microstructure to the effect that decreasing the processing speed and increasing the length of the die exit channel result in better homogeneity. Kim et al. [22] illustrated the corner gap formation between the die and work-piece during a plane strain simulation. They pointed out that the strain distribution of the work-piece became more inhomogeneous with a larger die corner gap. Also, the corner gap formation caused the strains in the outside region of the work-piece to reduce and simultaneously increase the strains in the inside region.

Unlike 2D simulations, there has been a few three dimensional FEM works on the ECAP process so far. Suo et al. [23] analyzed deformation heterogeneity during ECAP after one pass by using 3D FEM in three perpendicular planes of the billet. They demonstrated that equivalent plastic strains were not uniform in three directions. Jiang et al. [24] explored the strain distribution and working load of CP-Ti after four passes of ECAE by 3D FEM. It was obvious that the load increased with the number of ECAE passes. Djavanroodi et al. [25] designed an ECAP die based

on strain distribution uniformity. Their work presented that the $\Phi=120^0$and $\Psi=15^0$or 60^0 were the best die angles to achieve optimum strain dispensation homogeneity for the bulk of the sample. It was also shown that the values of $\Phi=60^0$ and $\Psi=15^0$ were optimum parameters for ECAP die based on the best strain distribution uniformity at the cross-section of the sample.

Furthermore, there are many experimental papers that state the influence of different parameters on mechanical properties obtained by the ECAP process. Several works were concentered on the effect of back pressure in ECAP [26-28]. These experimental works showed the positive role of back pressure such as the ability to achieve greater grain refinement, more homogeneous structure and workability of alloys processed by ECAP was enhanced. Furthermore, using backpressure caused more substantial enhancement in micro hardness term of the ECAPed samples. Several points with respect to temperature factor during the ECAP process were presented in some works [29-33]. First, there is a tendency for larger grains or sub grains to form at higher pressing temperatures. Second, the fraction of low-angle grain boundaries increased with increasing temperature. The examinations of the influence of the pressing speed demonstrated that the pressing speed had no significant effect on the equilibrium size of the ultrafine grains formed by ECAP [34-36]. Experiments were conducted by Nakashima et al. [37] to determine the impact of channel angle (Φ), using dies having channel angles from 90 to 157.5°. The experimental data expressed that an array of ultrafine equiaxed grains is achieved most easily when the sample is subjected to a very intense plastic strain using a die with $\Phi=90^0$.

As mentioned before, there are four basic processing routes in ECAP. The most published papers concluded that sub grains grow more rapidly into arrays of high angle boundaries using route B, less rapidly using route C and the evolution is slowest using route A [38, 39].

However, the role of the sample size, which is an important factor, has been reported just in few papers [40]. This parameter could be especially important in order to find out the possibility of using ECAP in industry. Horita et al. [40] presented mechanical properties of the AA1100 samples after six passes of ECAP and showed that mechanical properties were independent of the initial size. However, FEM simulations were not considered in their investigations.

The aim of the present paper is to experimentally and theoretically assess the effect of length and diameter of the ECAPed samples on mechanical properties, homogeneity of the microstructure and hardness variation. For this purpose, two dies with inside diameters of 10 and 20 mm were prepared for the ECAP process. The process was performed up to six passes on specimens with two different materials of pure copper and Al-Mg-Si 6012. The effective strain magnitude and homogeneity of strain on the cross-section of the samples were also studied by FEM and compared with experimental results. The experiments were repeated for 3 times in order to decrease the experiments errors.

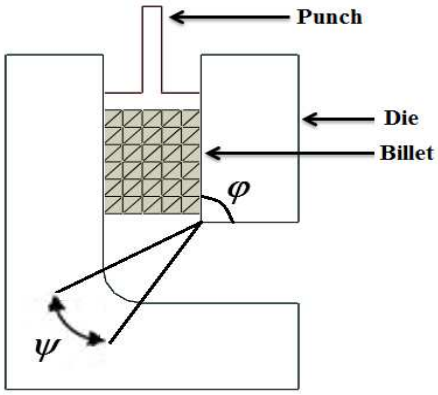

Figure 1. Schematic diagram of the ECAP die [41]

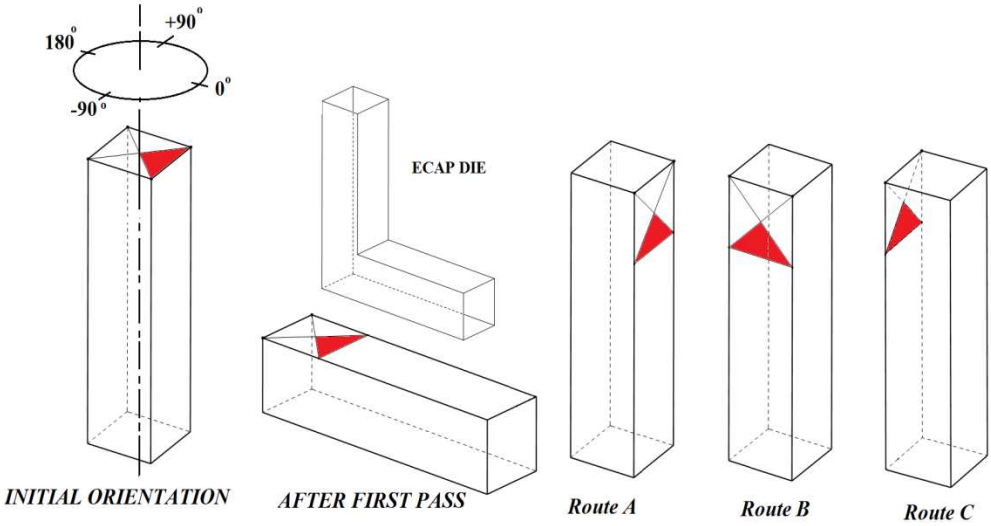

Figure 2. Four fundamental routes [41]

2. Experimental procedure

2.1 sample preparation

The experiments were conducted using rod-shaped samples of AA 6012 and pure copper of 99.97% and the chemical composition of them is represented in Tables 1 and 2, respectively.

Table 1. The chemical composition of commercial pure copper

Zn	Pb	Sn	P	Mn	Fe	Ni	Si	Mg	Cr	Sb
0.0023	0.0058	0.0055	< 0.0001	< 0.0002	0.0043	< 0.0020	< 0.0004	< 0.0001	< 0.0001	0.00011
Cd	**Bi**	**Co**	**Al**	**S**	**Be**	**Zr**	**B**	**Ti**	**Cu**	**As**
< 0.0001	0.0001	< 0.0006	< 0.0007	0.0012	< 0.0001	0.00037	< 0.0001	< 0.0001	99.976	< 0.0001

Table 2. The chemical composition of commercial AA6012

Al	**Si**	**Fe**	**Cu**	**Mn**	**Mg**	**Zn**	**Ni**	**Cr**	**Pb**	**Ti**	**Be**
rest	0.86	0.339	0.072	0.439	0.77	0.056	0.002	0.04	1.590	0.027	< 0.001
Ca	**Sr**	**Bi**	**V**	**Zr**	**Sn**	**Na**	**B**	**Ag**	**P**	**Co**	**Li**
0.001	< 0.001	0.001	0.004	0.002	0.002	0.001	0.003	< 0.001	0.005	< 0.001	0.055

The initial rods of AA6012 and pure copper were machined to samples with 10 and 20 mm in diameter and with lengths of 70 and 50 mm for each diameter. After that, the copper samples were annealed in a vacuum condition at 600 $^{\circ}$c for 2h and then cooled in the furnace. The Al samples were annealed at 430 $^{\circ}$c for 1h and then cooled down in air to room temperature.

2.2 Process parameters

The ECAP process was performed at room temperature (~22 °c) with a pressing speed of 2 $\frac{mm}{s}$. MoS2 was also used as lubrication. According to the literature, among the conventional routes A, B_C and C, route B_C is the most optimum processing route [38,39]. Therefore, six passes with route B_C were chosen in the experiments. Figure 3 shows the samples after the process. Two ECAP dies were designed and manufactured from the tool steel X153CrMoV12 and then hardened to 55 HRC. The channel angle 'Φ' and outer corner angle 'Ψ' of the both dies were 120° and 20°, respectively. However, they were different in channel diameter. The diameters of the die channels were 10mm and 20mm. The die geometry has a significant influence on the strain imposed on the sample in each pass. With regard to these values of Φ and Ψ the dies lead to the imposed strain of ~0.63 in each passage of sample through the die [7]. The hydraulic press and the ECAP dies set-up are shown in Figure 4

.

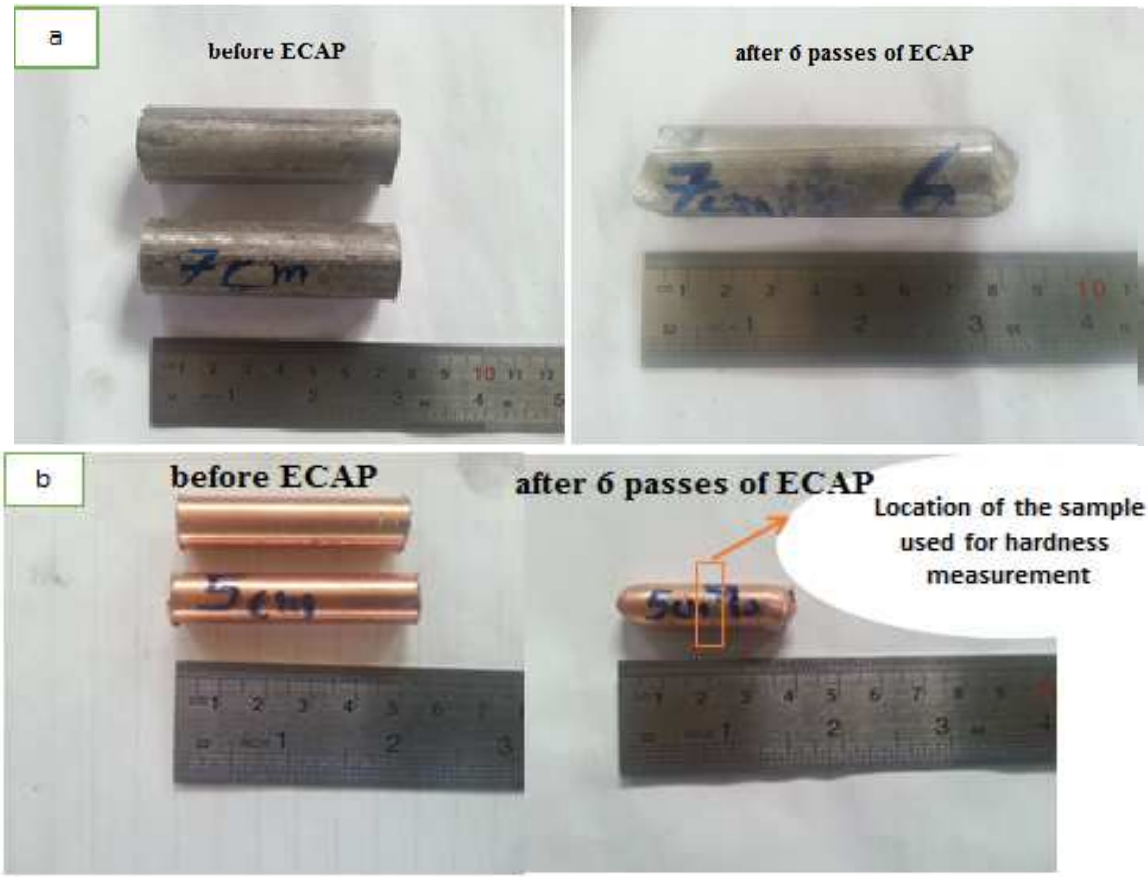

Figure 3. Billet after six passes a) AA 6012 with 20mm diameter and 70 mm length before and after 6 passes of ECAP b) Copper with 10mm diameter and 50 mm length before and after 6 passes of ECAP

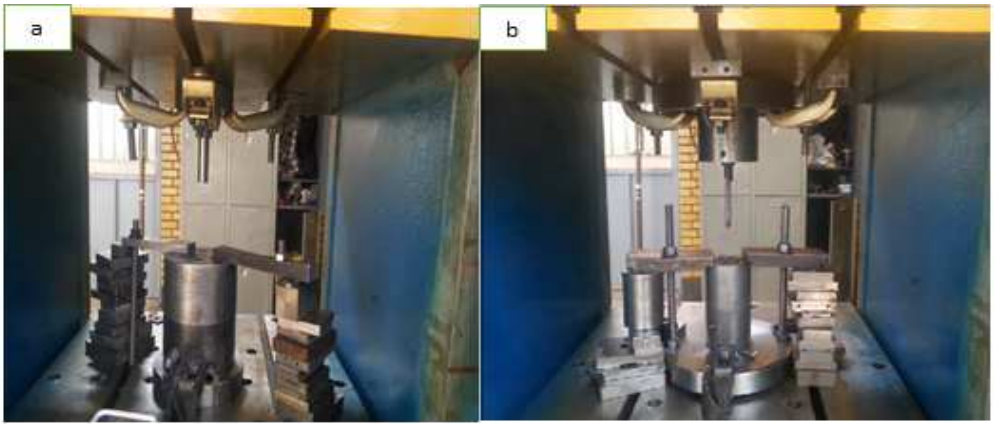

Figure 4. The ECAP set-ups for experimental work with channel diameters of: a) 20 mm b) 10 mm

After ECAP, the samples were sectioned perpendicular to the longitudinal axes in the middle of the billets, and then mounted. They were mechanically ground with SiC papers (grit 800-2500) and carefully polished with Al2O3 suspension to achieve a mirror-like surface finish. Micro hardness measurements were carried out by using micro hardness tester BUEHLER, equipped with a Vickers indenter. Results were recorded on each polished section across the width A-B, shown in Figure 5, with a distance of ~0.5 mm (for billets with diameters of 20mm) and ~0.25

mm (for billets with diameters of 10mm) between the indents. In other words, the hardness profile for each sample was composed of 40 points, regardless of the diameter size.

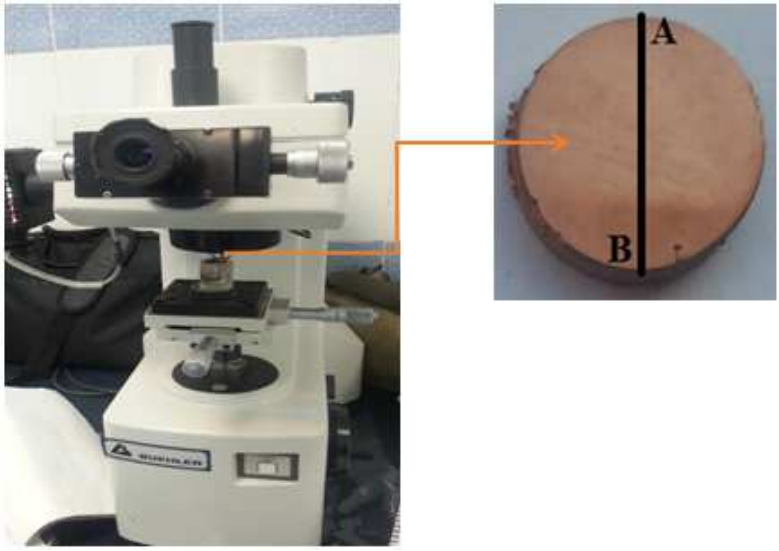

Figure 5. Micro hardness tester and cross section of the ECAPed sample

3. Experimental results

3.1. *Effects of billet geometry on microstructural homogeneity*

In order to evaluate the homogeneity of the microstructure, micro hardness profiles (Vickers Hardness) in the cross section of all the samples were plotted. For each sample, the measurements were repeated for three times. Figures 6 to 10 show the micro hardness profiles. There are two methods to quantify the degree of microhardness distribution homogeneity. One way is to use in homogeneity index (C_i) which is defined as follows [12] :

$$C_i = \frac{hardness_{max} - hardness_{min}}{hardness_{ave}} \quad (2)$$

Where $hardness_{max}$, $hardness_{min}$, and $hardness_{ave}$ express maximum, minimum and average hardness, respectively. As is obvious from Eq. (1), less magnitude of C_i leads to better hardness dispersal uniformity. According to Eq. (2), the second method is a mathematical coefficient named standard deviation (S.D). In this paper, both S.D and C_i are utilized to measure distribution uniformity.

$$S.D. = \sqrt{\frac{\sum_{i=1}^{n}(hardness_i - hardness_{ave})^2}{n}} \quad (3)$$

In Eq (2), n is the number of measured points.

Figure 6 shows the micro hardness profile across the line A-B for the annealed samples. The average measured hardness of annealed copper and AA6012 samples were 74 and 120, respectively.

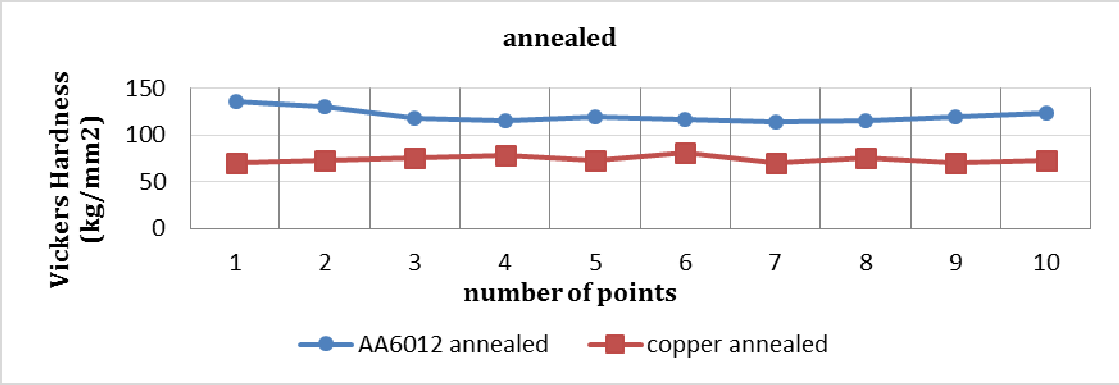

Figure 6. The profile of micro hardnesses in the cross section of the annealed samples

In Figure 7, the profile of the micro hardness in the cross section of the ECAPed AA6012 samples as well as their S.D and C index values are presented. The results of Figure 7 are for two billets of AA6012 with the identical diameter of 10 mm and different lengths of 50 and 70 (mm).The hardness average of the billet with 70 mm in length was 176. This amount was 173 for the billet with 50 mm in length. According to the average values of hardness's, the difference between them can be ignored.

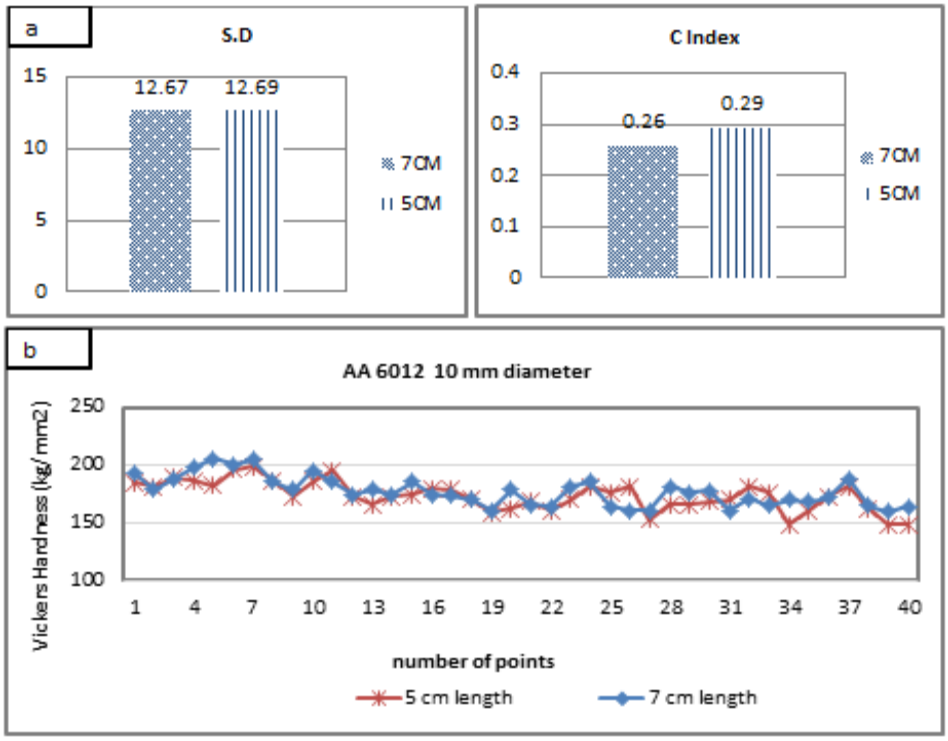

Figure 7. a) S.D and C index values of measured micro hardnesses b) the profile of micro hardness in the cross section of the AA6012 samples with ϕ =10mm and lengths of 70 and 50 mm

Corresponding to Figure 7, Figure 8 shows the same results for copper samples. The hardness average of the billet with 70 mm in length was 147. This amount was 150 for the billet with 50 mm in length. Similar to the AA6012 samples, the difference between the values is very small and can be ignored.

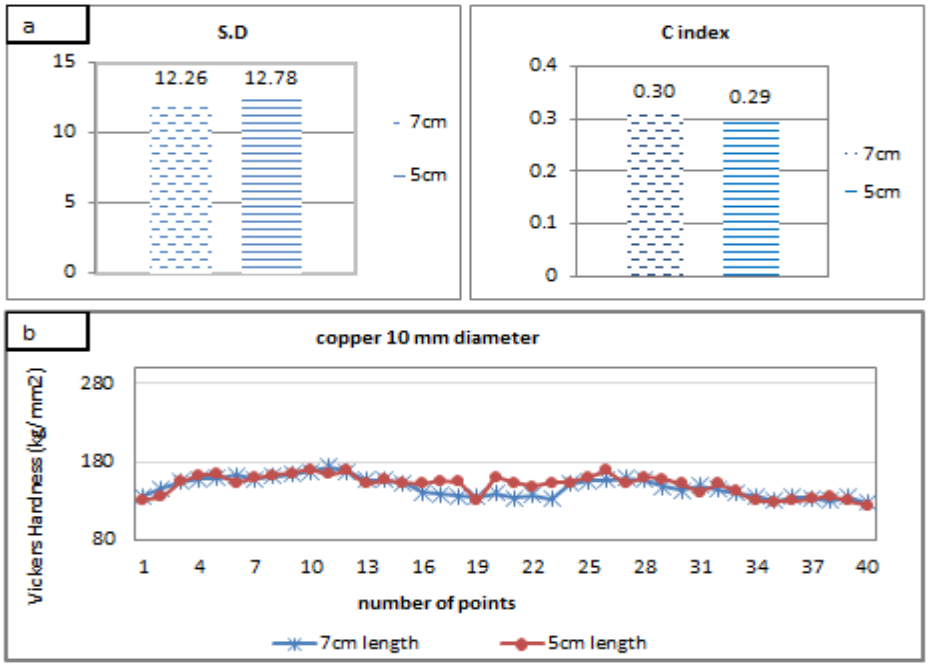

Figure 8. a) S.D and C index values of measured micro hardnesses b) the profile of micro hardness in the cross section of the copper samples with ϕ =10mm and lengths of 70 and 50 mm

Figure 9 and Figure 10 show the similar results for samples with 20mm in diameter and different length of 70 and 50mm. The hardness average of the AA6012 billet with 70 mm in length was 169. This amount was 167 for the billet with 50 mm in length. These values are 144 (L=70mm) and 145 (L=50mm) for copper samples.

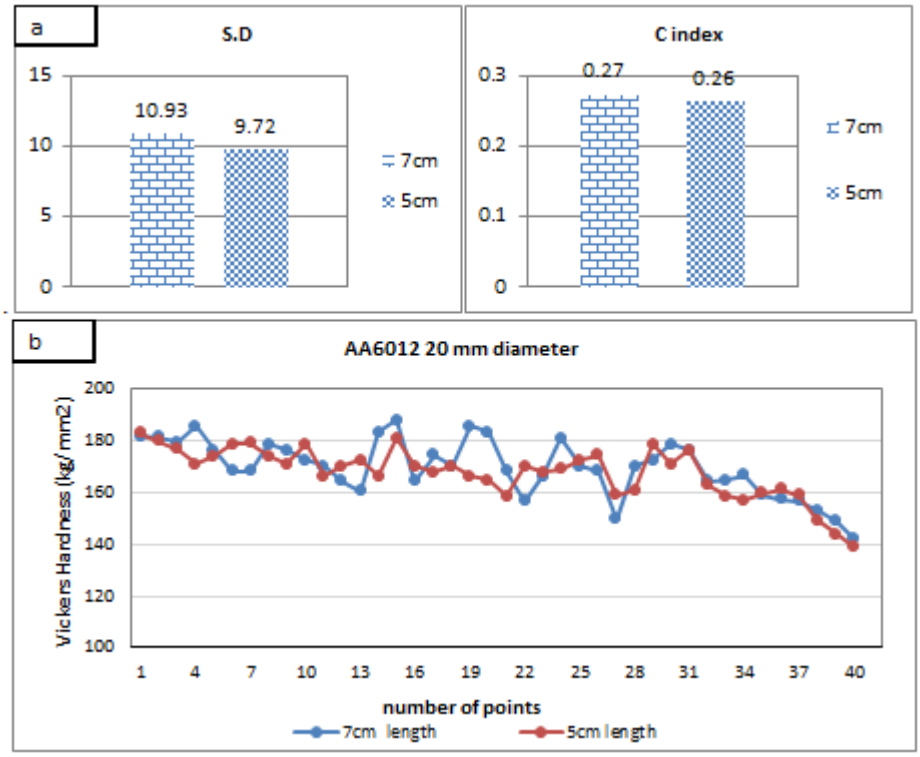

Figure 9. a) S.D and C index values of measured micro hardnesses b) the profile of micro hardness in the cross section of the AA6012 samples with ϕ =20mm and lengths of 70 and 50 mm

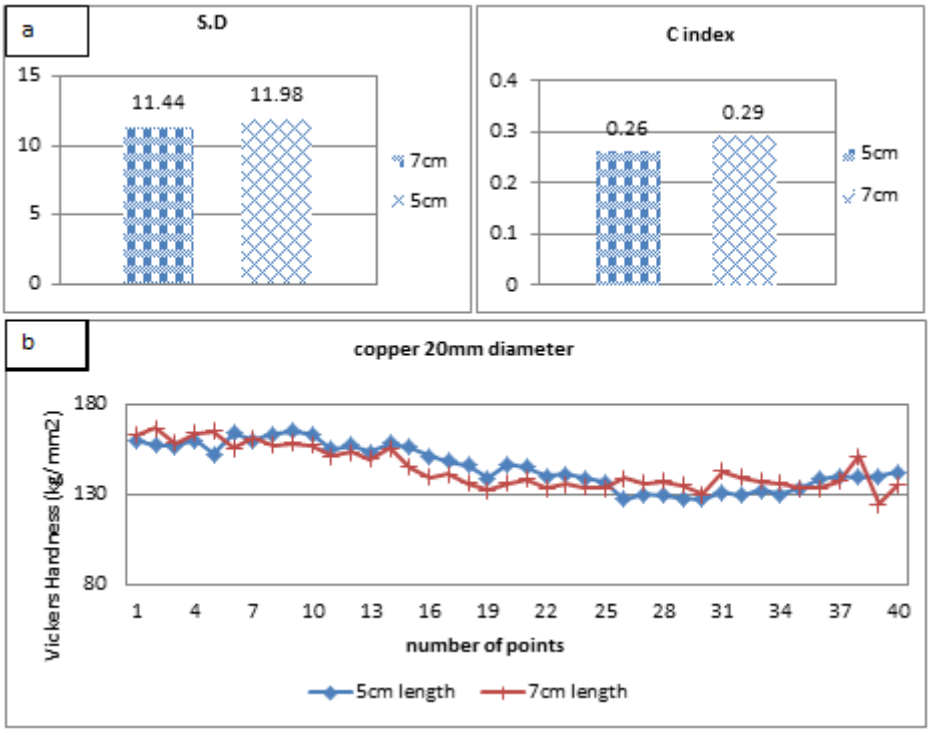

Figure 10. a) S.D and C index values of measured micro hardnesses b) the profile of micro hardness in the cross section of the copper samples with ϕ =20mm and lengths of 70 and 50 mm

3.2. Tensile test

In order to measure tensile strengths and deformation behavior of the samples, tensile tests of the annealed and ECAPed samples were carried out at room temperature with the speed of 2 $\frac{mm}{min}$. The tests were performed by Hounsfield-H50ks tester equipped with a computer controller. Each Ecaped sample was prepared according to ASTM-EM8. Figure 11 shows the tensile tester. Table 3 presents the yield strengths, ultimate tensile strengths of pure copper and AA6012 samples before and after the ECAP process.

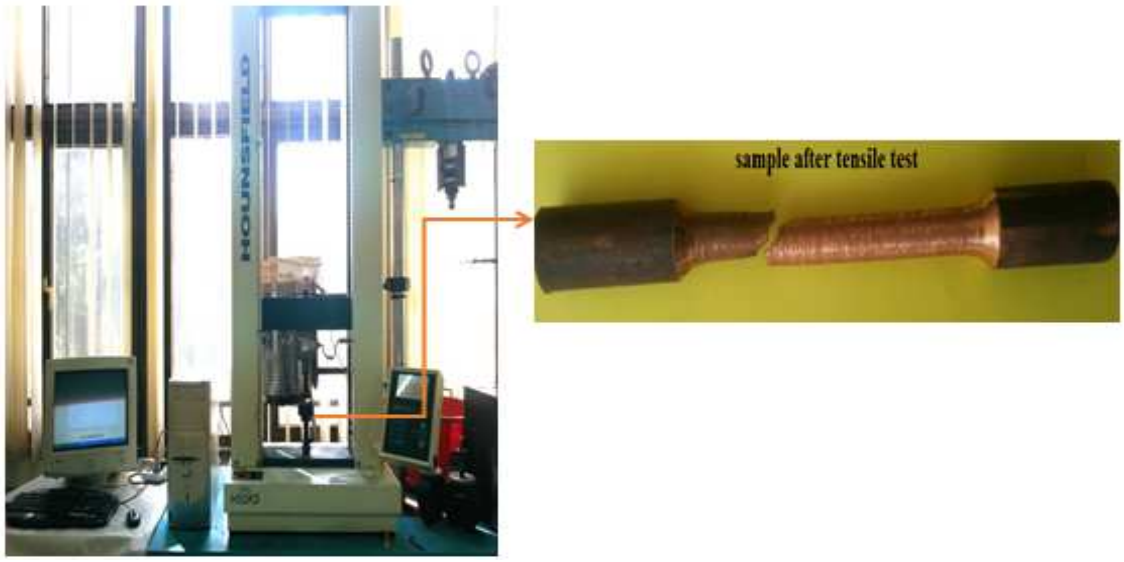

Figure 11. Tensile tester used in this study

Table 3. Mechanical properties of the samples before and after six passes of ECAP

sample	Annealed copper	ECAPed copper ϕ =10mm	ECAPed copper ϕ =20mm	annealed AA6012	ECAPed AA6012 ϕ =10mm	ECAPed AA6012 ϕ =20mm
σ_{yp}(MPa)	57.05	213.5	216.8	39.4	137.5	144.2
σ_{UTS}(MPa)	215.99	460.7	465.5	184.3	266.6	276

4. Discussion

4.1 Hardness and tensile test Evaluations

The variations of average Vickers micro hardness (HV) before and after six passes of ECAP on the AA6012 and pure copper samples were presented in the results section. The HV magnitudes of AA6012 samples with 10 mm in diameter were 120 before ECAP, 176 after ECAP of billets with 70mm in length and 173 after ECAP of billets with 50mm in length. It can be concluded that length has no significant effect on the average hardness after the ECAP process. However, applying severe plastic deformation led to significant improvements at the HV values. It was found that an enhancement of almost 45% after the sixth pass has been achieved for AA6012 specimens with 10 mm in diameter.

The HV magnitudes of AA6012 samples with 20 mm in diameter were 120 before ECAP, 169 after ECAP of billets with 70mm in length and 167 after ECAP of billets with 50mm in length. It means that an improvement of almost 39% in average hardness was obtained. As a matter of fact, there is no difference between two specimens that had diverse length and same diameter but there was an important diversity in homogeneity of two billets that had diameters of 10 and 20 mm. As can be seen, the sample with bigger diameter becomes more homogeneous (about 13%).

The HV magnitudes of the copper samples with 10 mm in diameter were 74 before ECAP and almost 148 after ECAP of the billets with 70 and 50 mm in length. It shows that an improvement of 100% in average hardness was obtained. The HV magnitudes of the copper samples with 20 mm in diameter were 145 after ECAP. It was apparent that the ECAP process caused 96% increase in hardness magnitude of the copper samples with 20 mm in diameter after six passes of ECAP. The length had no noticeable effect on the HV values like the AA6012 samples. Also, there was an important diversity in homogeneity of two billets that had diameters of 10 and 20 mm. As can be seen, the sample with bigger diameter becomes more homogeneous (about 11%).

Tensile tests showed that the yield strength of pure copper sample increased by about 274% for 10 mm diameter and 280% for 20mm diameter. Furthermore, ultimate tensile strengths were enhanced about ~ 115% and therefore the yield strength (σ_y) had a higher increasing rate. In addition, after six passes of ECAP on AA6012 the values of yield strength increased about 248% and 265% for specimens of 10 and 20mm diameters. Also, almost 45% and 50% enhancements in magnitudes of ultimate tensile strength of 10 and 20mm diameter were observed. Thus, yield

strength had more noticeable improvement in increasing rate. As can be observed, larger billets had more values in ultimate tensile strength and yield point.

4.2 Finite element modelling

For this study, finite element methods were also carried out using abaqus /Explicit. The dies and punchs were assumed to be rigid without any deformation. The simulation conditions were considered to be the same as the experiments. For all the simulations, the friction cofficient of 0.05 was used. In order to decrease the time of the simulations, symmetrical boundry condition was applied and only half portion of the dies and samples were considered for analysis as shown in Figure 12. The effective strain variations across the width A–B, shown in Figure 13, were taken to compare with the corresponding hardness values obtained from experiments.

The effective strain contours in the middle cross section (line A-B) of the different ECAPed samples are shown in Figures 13-16. It should be noted that one pass of ECAP was considered in the simulations. The previous parameter of S.D was also used to evaluate the results.

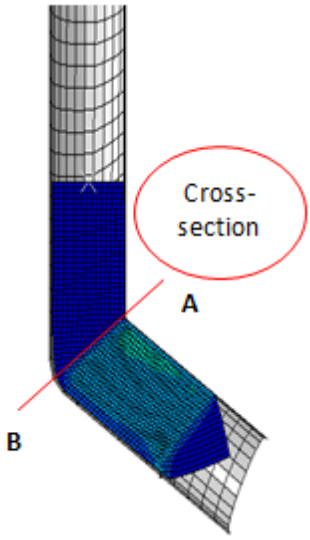

Figure 12. Die and the internal surface used for meshing

The contours shown in Figure 13 are for two AA6012 speimens with the same diamaters of 10mm but different lengths of 70mm and 50mm. the average strain of both samples is ~ 0.59. According to the S.D values, starin ditribution is almost the same for them as can be seen in Figure 13 .

Figure 14 shows the effective strain contours in the middle section of two pure copper speimens with the same diamaters of 10mm but different lengths of 70mm and 50mm. the average strain of both samples are ~ 0.58. According to the S.D values, starin ditribution is analogous to the AA6012 specimmens. Hence, simulations did not show noticeable difference in strain homogeneity for samples with the same diameters and different lengths. This result was also achieved in evaluating hardness values.

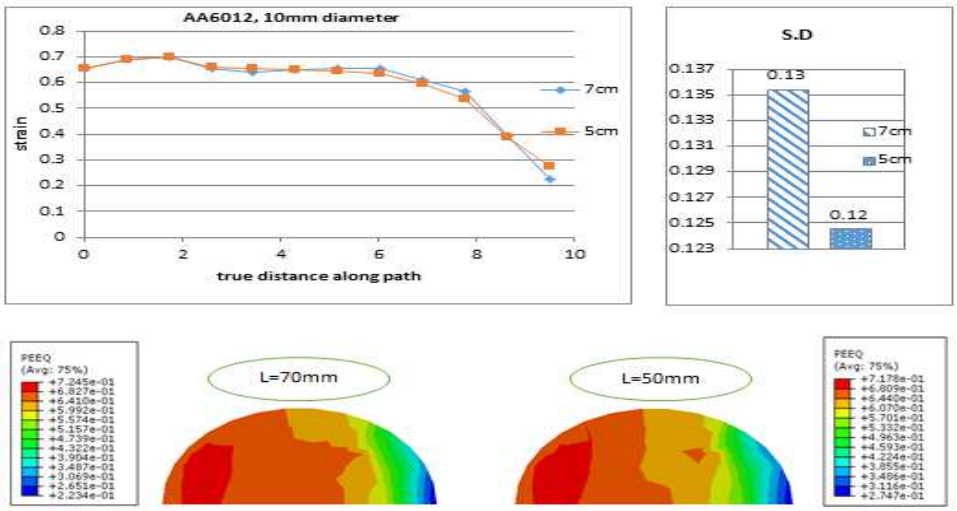

Figure 13. 3D shapes and effective strain contours across width A–B for the AA6012 samples with 10mm in diameter and different lengths of 70 and 50mm, after one pass of the ECAP process

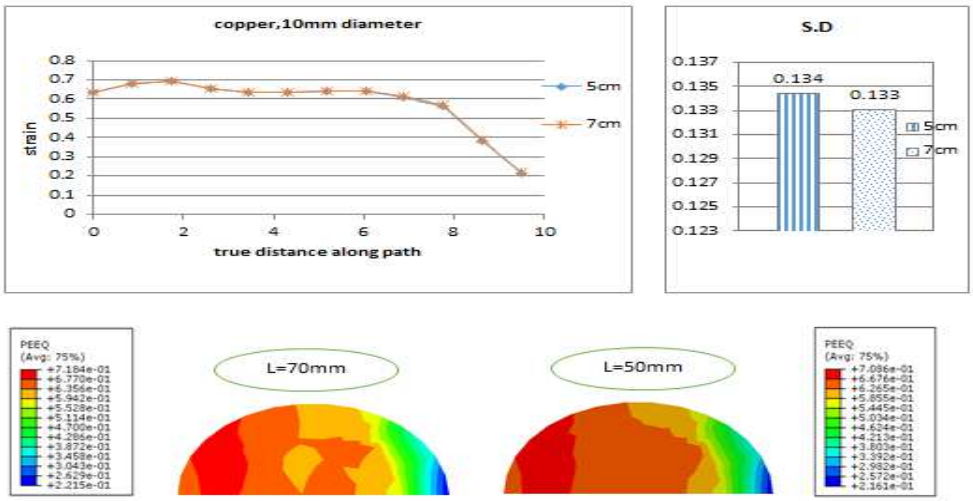

Figure 14. 3D shapes and effective strain contours in width A–B the copper samples wih 10mm diameter and different lengths after the ECAP process

Figure 15 shows the effective strain contours in the middle section of two AA6012 speimens with the same diamaters of 20mm but different lengths of 70mm and 50mm. the average strain of both samples are ~ 0.54. Figure 16 also shows these results for the copper specimens with the same diamater of 20mm and different lengths of 70mm and 50mm.By comparing the SD values of effective strains between the samples with different diamaters of 10 mm and 20mm, it can be conlcuded that the samples with larger diameter had better homogenity of strain in their cross sections. The homogenity of the effective strains in the cross sections of the samples with diamters of 20 mm improved by ~38% in comparison with the samples with diamters of 10mm. This result was also achieved from the hardness measuerments in the experiments. The homogenity of the hardness values in the cross sections of the samples with diamters of 20 mm improved by ~23% and 8% in comparison with the AA6012 and copper samples with diamters of 10mm, respectively. Although the amount of improvement was different in the copper samples, it was concluded that samples with larger diameters have better homogenity of the produced structure after the ECAP process.The results of the simulations were in good agreement with

experimental results. Both of them showed identical homogeneity for billets with the same diameters and different length. Moreover, both simulations and experimental data showed a noticeable difference in homogeneity between billets with different diameters.

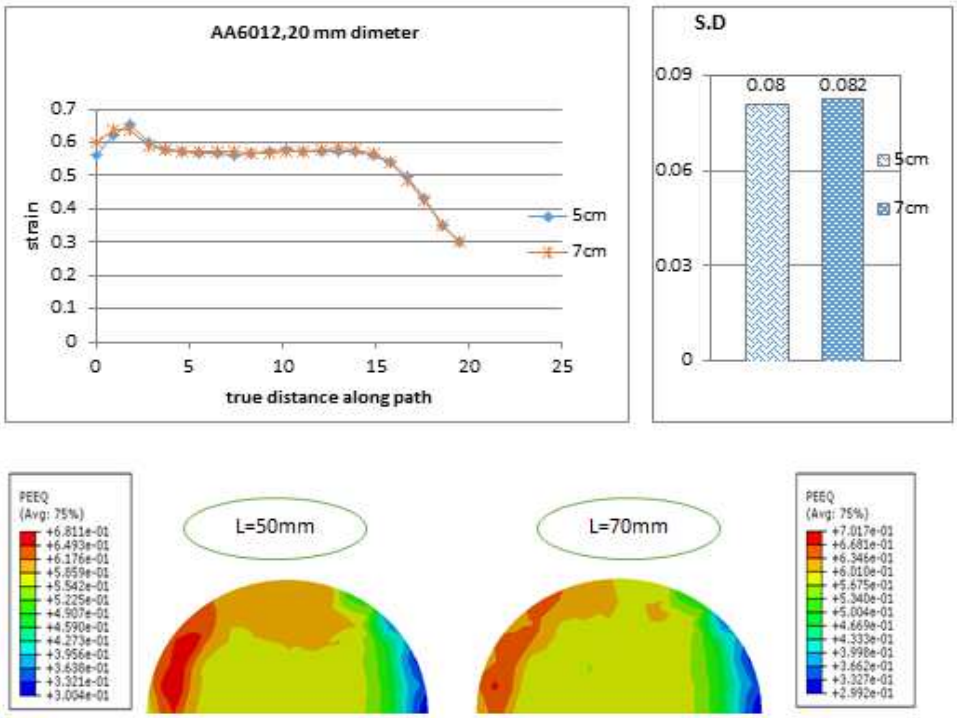

Figure. 15. 3D shapes and effective strain contours in width A–B the copper samples wih 10mm diameter and different lengths after the ECAP process

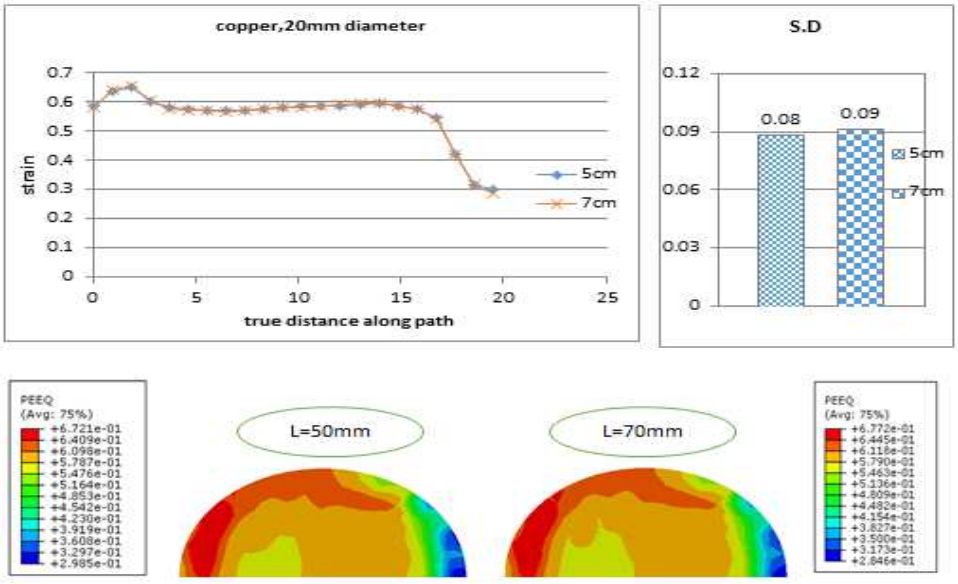

Figure 16. 3D shapes and effective strain contours in width A–B the copper samples wih 10mm diameter and different lengths after the ECAP process

5. Coclusion

The effects of material properties and billet geometry were investigated by experimental and FEM method. Investigations were made after six passes of ECAP and using route B_C for pure commercial copper and AA6012. The following conclusions were obtained:

1. Diameter plays an important role in the ECAP process in effective strain values and homogeneity. In addition, reducing the height had no effect on homogeneity of structure.
2. To validate the simulation results, experimental values were compared with simulation data and there was a good agreement between them. Since increasing the sample diameter resulted in more homogeneity of effective strain as well as hardness distribution in the cross-section of the samples,it can be concluded that the ECAP process could be more effective on the billet with larger diameter with regard to homogeneity of structure.
3. During the ECAP process, dislocation pile up at the border of the grains has increased and consequently made smaller grain size.Therefore, higher values of HV and mechanical properties were observed. Hardness measuring of the ECAPed samples of AA6012 and copper showed that the hardness values were about 1.46 and 2.02 times higher than that of the annealed samples, respectively. Moreover, tensile tests of the specimens showed an increase of 115% in ultimate tensile strength of copper and 50% in AA6012 after six passes of ECAP .
4. After six passes of ECAP, an increase of 102% in hardness for the copper samples and an increas of 45% for the AA6012 samples were observed.
5. The variation in hardness magnitude was very small when the diameter became larger.
6. The hardness homogeneity of the samples with larger diameteres were better in comparsion with the smaller diameters. The homogenity of the samples with diamater of 20 mm after six passes of ECAP improved about 23% for the AA6012 samples and 8% for the copper samplesin comparision with the samller diamater samples (D=10mm).
7. FEM simulations were carried out corressponding to the experimental conditions. The FEM results were in good agreement with the experimental data such that both of them had the same conclusions with respect to the geometric effect in the ECAP process.
8. It could be said that ECAP can be used for larger billets and will be useful in industrial works.

6. References

[1] Stolyarov, V.V., et al. 2001. Influence of ECAP routes on the microstructure and properties of pure Ti. Materials Science and Engineering: A, 299(1–2), 59-67.

[2] Valiev, R., et al. 2006. Producing bulk ultrafine-grained materials by severe plastic deformation. JOM, 58(4), 33-39.

[3] VM., S., et al., Russian Metall. 1981, 1-99.

[4] Borodachenkova, M., et al. 2013. Severe plastic deformation of AL-ZN alloys: experimental analysis and modeling.
[5] Segal, V. 1999. Equal channel angular extrusion: from macro mechanics to structure formation. Materials Science and Engineering: A, 271(1), 322-333.
[6] Langdon, T.G. 2007. The principles of grain refinement in equal-channel angular pressing. Materials Science and Engineering: A, 462(1-2), 3-11.
[7] Furukawa, M., et al. 1996. Microstructural characteristics of an ultrafine grain metal processed with equal-channel angular pressing. Materials characterization, 37(5), 277-283.
[8] Sordi, V.L., et al. 2014. Experimental and FEM Studies of the Relationships between Equal-Channel Angular Pressing Die Design, Strain Distribution and Pressing Forces. in Advanced Materials Research. Trans Tech Publ.
[9] Kim, H.S. 2001. Finite element analysis of equal channel angular pressing using a round corner die. Materials Science and Engineering: A, 315(1), 122-128.
[10] Srinivasan, R. 2001. Computer simulation of the equichannel angular extrusion (ECAE) process. Scripta Materialia, 44(1), 91-96.
[11] Yang, Y.L. and Lee, S. 2003. Finite element analysis of strain conditions after equal channel angular extrusion. Journal of Materials Processing Technology, 140(1), 583-587.
[12] Li, S., et al. 2004. Finite element analysis of the plastic deformation zone and working load in equal channel angular extrusion. Materials Science and Engineering: A, 382(1), 217-236.
[13] Pérez, C.L. 2004. On the correct selection of the channel die in ECAP processes. Scripta Materialia, 50(3), 387-393.
[14] Lu, S.K., et al. 2011. 3D FEM simulations for the homogeneity of plastic deformation in aluminum alloy HS6061-T6 during ECAP. Procedia Engineering, 12(0), 35-40.
[15] Esmailzadeh, M. and Aghaie-Khafri, M. 2012. Finite element and artificial neural network analysis of ECAP. Computational Materials Science, 63(0), 127-133.
[16] Kim, H.S., Seo, M.H. and Hong, S.I. 2001. Plastic deformation analysis of metals during equal channel angular pressing. Journal of Materials Processing Technology, 113(1), 622-626.
[17] Han, J. H., et al. 2009. Effects of die geometry on variation of the deformation rate in equal channel angular pressing. Metals and Materials International, 15(3), 439-445.
[18] Nagasekhar, A., et al. 2005. Effect of acute tool-angles on equal channel angular extrusion/pressing. Materials Science and Engineering: A, 410, 269-272.
[19] Oruganti, R.K., et al. 2005. Effect of friction, backpressure and strain rate sensitivity on material flow during equal channel angular extrusion. Materials Science and Engineering: A, 406(1–2), 102-109.
[20] Xu, S., et al. 2007. Finite element analysis and optimization of equal channel angular pressing for producing ultra-fine grained materials. Journal of Materials Processing Technology, 184(1), 209-216.
[21] Yoon, S.C., Nagasekhar, A.V. and Kim, H.S. 2009. Finite element analysis of the bending behavior of a workpiece in equal channel angular pressing. Metals and Materials International, 15(2), 215-219.
[22] Kim, H.S., Seo, M.H. and Hong, S.I. 2000. On the die corner gap formation in equal channel angular pressing. Materials Science and Engineering: A, 291(1), 86-90.

[23] Suo, T., et al. 2006. The simulation of deformation distribution during ECAP using 3D finite element method. Materials Science and Engineering: A, 432(1–2), 269-274.
[24] Jiang, H., Fan, Z. and Xie, C. 2008. 3D finite element simulation of deformation behavior of CP-Ti and working load during multi-pass equal channel angular extrusion. Materials Science and Engineering: A, 485(1–2), 409-414.
[25] Djavanroodi, F., et al. 2012. Designing of ECAP parameters based on strain distribution uniformity. Progress in Natural Science: Materials International, 22(5), 452-460.
[26] Stolyarov, V.V. and Lapovok, R. 2004. Effect of backpressure on structure and properties of AA5083 alloy processed by ECAP. Journal of Alloys and Compounds, 378(1–2), 233-236.
[27] Xu, C., Xia, K. and Langdon, T.G. 2007. The role of back pressure in the processing of pure aluminum by equal-channel angular pressing. Acta Materialia, 55(7), 2351-2360.
[28] Xu, C., Xia, K. and Langdon, T.G. 2009. Processing of a magnesium alloy by equal-channel angular pressing using a back-pressure. Materials Science and Engineering: A, 527(1–2), 205-211.
[29] Yamashita, A., et al. 2000. Influence of pressing temperature on microstructural development in equal-channel angular pressing. Materials Science and Engineering: A, 287(1), 100-106.
[30] Shin, D.H., et al. 2002. WITHDRAWN: Effect of pressing temperature on microstructure and tensile behavior of low carbon steels processed by equal channel angular pressing. Materials Science and Engineering: A, 325(1), 31-37.
[31] Chen, Y., et al. 2003. The effect of extrusion temperature on the development of deformation microstructures in 5052 aluminium alloy processed by equal channel angular extrusion. Acta Materialia, 51(7), 2005-2015.
[32] Goloborodko, A., et al. 2004. Effect of pressing temperature on fine-grained structure formation in 7475 aluminum alloy during ECAP. Materials Science and Engineering: A, 381(1), 121-128.
[33] Wang, Y., et al. 2004. Effect of deformation temperature on the microstructure developed in commercial purity aluminum processed by equal channel angular extrusion. Scripta materialia, 50(5), 613-617.
[34] Berbon, P.B., et al. 1999. Influence of pressing speed on microstructural development in equal-channel angular pressing. Metallurgical and Materials Transactions A, 30(8), 1989-1997.
[35] Yamaguchi, D., et al. 1999. Significance of adiabatic heating in equal-channel angular pressing. Scripta materialia, 41(8), 791-796.
[36] Kim, I., et al. 2003. Effects of grain size and pressing speed on the deformation mode of commercially pure Ti during equal channel angular pressing. Metallurgical and Materials Transactions A, 34(7), 1555-1558.
[37] Nakashima, K., et al. 1998. Influence of channel angle on the development of ultrafine grains in equal-channel angular pressing. Acta materialia, 46(5), 1589-1599.
[38] Iwahashi, Y., et al. 1998. The process of grain refinement in equal-channel angular pressing. Acta Materialia, 46(9), 3317-3331.
[39] Oh-Ishi, K., et al. 1998. Optimizing the rotation conditions for grain refinement in equal-channel angular pressing. Metallurgical and Materials Transactions A, 29(7), 2011-2013.

[40] Horita, Z., Fujinami, T. and Langdon, T.G. 2001. The potential for scaling ECAP: effect of sample size on grain refinement and mechanical properties. Materials Science and Engineering: A, 318(1), 34-41.

[41] Ahmadi, F. and Farzin, M. 2014. Investigation of a new route for equal channel angular pressing process using three-dimensional finite element method. Proceedings of the Institution of Mechanical Engineers, Part B: Journal of Engineering Manufacture, 228(7), 765-774.